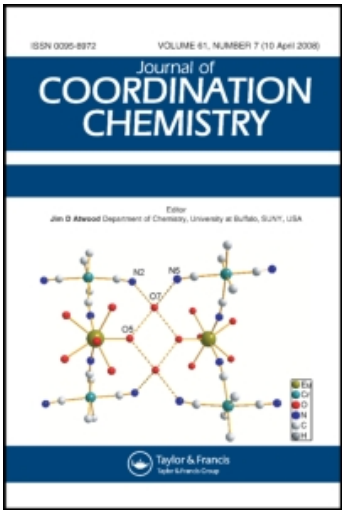

Journal of Coordination Chemistry
Publication details, including instructions for authors and subscription information:
http://www.informaworld.com/smpp/title~content=t713455674

UTILIZATION OF CHEMICAL AND STRUCTURAL CHARACTERISTICS OF TETRAAZA CYCLOALKANE COMPLEXES

Tasuku Ito[a]; Masako Kato[a]; Masahiro Yamashita[a]; Haruko Ito[a]
[a] Department of Applied Molecular Science, Institute for Molecular Science, Okazaki National Research Institutes, Myodaiji, Okazaki, Japan

To cite this Article Ito, Tasuku , Kato, Masako , Yamashita, Masahiro and Ito, Haruko(1986) 'UTILIZATION OF CHEMICAL AND STRUCTURAL CHARACTERISTICS OF TETRAAZA CYCLOALKANE COMPLEXES', Journal of Coordination Chemistry, 15: 1, 29 — 52
To link to this Article: DOI: 10.1080/00958978608075854
URL: http://dx.doi.org/10.1080/00958978608075854

J. Coord. Chem., 1986, Vol. 15, pp. 29–52
0095-8972/86/1501-0029 $18.50/0

UTILIZATION OF CHEMICAL AND STRUCTURAL CHARACTERISTICS OF TETRAAZA CYCLOALKANE COMPLEXES

TASUKU ITO†, MASAKO KATO, MASAHIRO YAMASHITA

and

HARUKO ITO

Department of Applied Molecular Science, Institute for Molecular Science, Okazaki National Research Institutes, Myodaiji, Okazaki 444, Japan

(Received April 16th, 1985)

The research investigations aiming at taking advantage of the chemical and structural consequences of ligand macrocyclization are reviewed with regard to the three features as follows: (1) Tetraazacycloalkane complexes which take up carbon dioxide as $ROCO_2^-$ or $R_2NCO_2^-$; (2) Correlation between axial and in-plane coordination bond lengths in tetragonal six-coordinate complexes of the *trans*-MX_2N_4-type ($M=Co^{3+}$, Ni^{2+}, and Zn^{2+})-X-ray structural and *ab initio* MO studies and (3) Stabilization of high oxidation states of metal ions and its application to chemistry of one-dimensional halogen-bridged M^{2+}-M^{4+} mixed valence complexes.

1. INTRODUCTORY REMARK

During the past 20 years, coordination chemistry of macrocylic compounds has undergone spectacular growth. In the early stage of the expansion, the main goal was the analogy between synthetic macrocyclic compounds and many natural product systems. But more recently, the emphases of reported research have been ranged over the whole spectrum of chemistry. We describe herein novel chemistry of macrocyclic complexes developed mainly in our laboratory. The chemistry is achieved by taking advantage of chemical consequences of ligand macrocyclization.

Structures of tetraazamacrocyclic ligands used in this study are shown below along with ligand abbreviations.

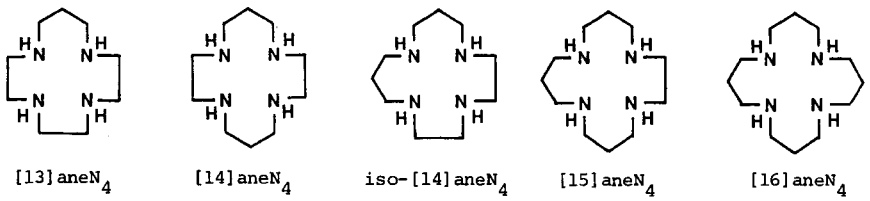

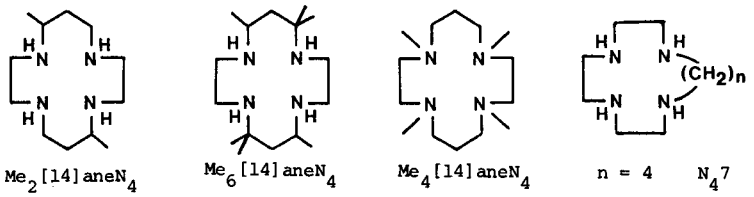

2. TETRAAZACYCLOALKANE COMPLEXES WHICH TAKE UP CO_2 AS $ROCO_2^-$ OR $R_2NCO_2^-$

2.1 Introduction

Coordination of CO_2 to a transition metal complex and reactions of the resulting complex have been of interest in connection with the utilization of CO_2.[1] Besides direct coordination of CO_2 to transition metals with its intact form,[2] many insertion reactions of CO_2 into an M-X bond (X= H, C, O, N) have been reported.[3] We have found a new system[4] of divalent metal complexes containing tetraazacycloalkanes (L) shown previously, which take up CO_2 as $ROCO_2^-$, $RR'NCO_2^-$, or HCO_3^-.

The CO_2 up-take reactions described herein are of the type such that tetraaza macrocyclic complexes (ML^{2+}) take up $ROCO_2^-$, $R_2NCO_2^-$, or $HOCO_2^-$, which has been produced from CO_2 in solution in the presence of base (B). The reaction involves the increase in coordination number of the metal ion from 4 to 5 or 6 and is described as follows.

$$ML^{2+} + CO_2 + XH \xrightarrow[B]{} M(O_2CX)(L)^+ + BH^+ \qquad (1)$$

where XH = ROH, R_2NH, or H_2O. The starting complex ML^{2+} is of the square-planar type, while the coordination geometry of the resulting complex is octahedral or trigonal bipyramidal. The coordinatively unsaturated nature of ML^{2+} complexes makes this type of reactions possible. We have studied complexes of Ni^{2+}, Zn^{2+}, and Cd^{2+} which often show the required coordination behavior. As to the effect of base (B) in Eq. (1), there was no difference between NaOR and NEt_3, the former of which has a coordinating anion whereas that of the latter is difficult to coordinate to a metal ion. Therefore, base (B) is considered to play the role of increasing the concentration of XCO_2^- in solution according to Eq. (2).

$$\begin{aligned} &XH = ROH: \; ROH + CO_2 + B \rightleftharpoons ROCO_2^- + BH^+ \\ &XH = R_2NH: \; R_2NH + CO_2 + B \rightleftharpoons R_2NCO_2^- + BH^+ \\ &XH = H_2O: \; H_2O + CO_2 + B \rightleftharpoons HOCO_2^- + BH^+ \end{aligned} \qquad (2)$$

2.2 Formation of $M(L)(O_2CX)^+$ Complexes

2.2.1 Monoalkylcarbonato complexes (XH = ROH)[4a] When a stream of CO_2 is passed through a methanolic solution containing equimolar amounts of $Zn(ClO_4)_2 \cdot 6H_2O$ and L at room temperature, Zn^{II}-monomethylcarbonato complexes with L are obtained (Scheme I). When CO_2 is not admitted, only $Zn(L)(ClO_4)_2$ is isolated. However, the resulting $Zn(L)(ClO_4)_2$ also reacts with CO_2 in CH_3OH at room temperature to give $Zn(L)(O_2COCH_3)(ClO_4)$. In general, addition of a small amount of base such as $NaOCH_3$ or NEt_3 facilitates the CO_2 uptake markedly. As shown in Scheme I, the reaction with CO_2 is reversible. When a methanolic solution of $Zn(L)(O_2COCH_3)(ClO_4)$ is purged with a stream of N_2 or is allowed to warm to *ca* 40°C, $Zn(L)(ClO_4)_2$ is produced again.

Scheme I

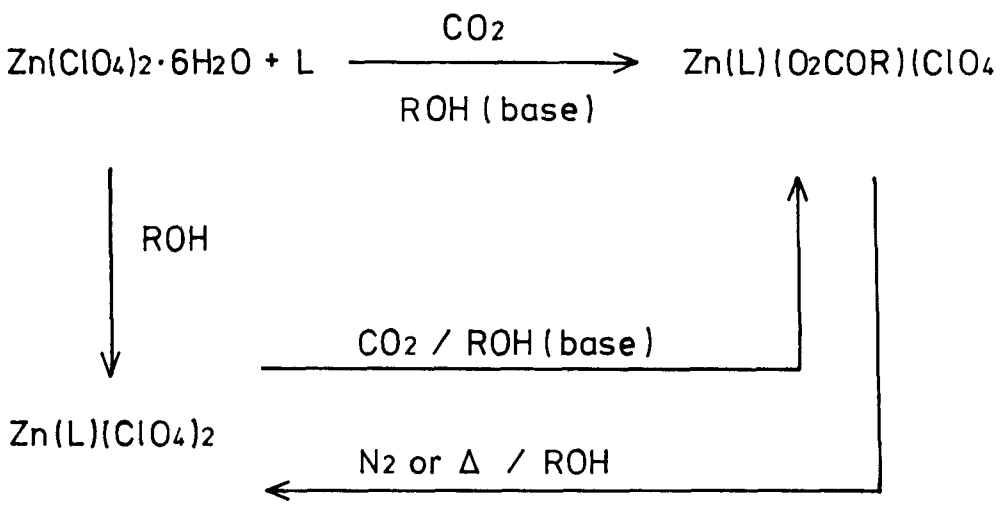

Ni^{II}- and Cd^{II}-O_2COR complexes were prepared from $[ML](ClO_4)_2$ in a similar way. Table I lists the $ROCO_2^-$ complexes synthesized in this study.

TABLE I
List of $M(L)(O_2CX)^+$ prepared and characterized†

$ROCO_2^-$ Complexes	
$Zn(L)(O_2COR)(ClO_4)$	$Ni(L)(O_2COR)(ClO_4)$
L=[14]aneN$_4$: R=Me‡, Et	L=[14]aneN$_4$: R=Me
L=[15]aneN$_4$: R=Me, Et	L=[15]aneN$_4$: R=Me
L=Me$_2$[14]aneN$_4$: R=Me	L=TMC : R=Me‡
L=TMC : R=Me‡, Et	L=iso-[14]aneN$_4$: R=Me
L=iso-[14]aneN$_4$: R=Me	
$\{Zn(L)\}_3(O_2COR)_2(ClO_4)_4$	$Ni(L)(H_2O)(O_2COR)(ClO_4)$
L=[15]aneN$_4$: R=Me‡, n-Bu	L=CTH : R=Me, Et
$Cd(L)(O_2COR)(ClO_4)$	$Ni(L)(O_2COR)_2$
L=TMC : R=H‡, Me‡	L=TMC : R=Me‡
$R_2NCO_2^-$ Complexes	
$Zn(L)(O_2CNR_2)(ClO_4)$	$Ni(L)(O_2CNR_2)(ClO_4)$
L=TMC : R=Me, Et	L=TMC : R=Me, Et
	L=CTH : R = Me, Et‡, n-Pr, n-Bu
$Cd(L)(O_2CNR_2)(ClO_4)$	
L=TMC : R=Me, Et	

† TMC and CTH stand for Me_4[14]aneN$_4$ and rac-Me_6[14]aneN$_4$, respectively.
‡ X-ray structure available.

Particularly fascinating characteristics of this system are that the CO_2 uptake reactions proceed under very mild conditions and that, in certain cases (e.g. Zn^{II}-[14]aneN$_4$, Zn^{II}-[15]aneN$_4$ systems), CO_2 is taken up spontaneously from the air without bubbling CO_2.

2.2.2 Carbamato complexes (XH = R_2NH) For the preparation of the carbamato complex $M(L)(O_2CNR_2)^+$, we used as tetraazacycloalkane *rac*-Me$_6$[14]aneN$_4$ (7SR, 14SR-form) and Me$_4$[14]aneN$_4$ (TMC). They are known to fold readily to afford five or six-coordinate complexes. There are two synthetic routes, A and B.

$$(A)\quad ML^{2+} + CO_2 + 2R_2NH \longrightarrow M(O_2CNR_2)L^+ + NH_2R_2$$

$$(B)\quad M(O_2CX)L^+ + R_2NH \longrightarrow M(O_2CNR_2)L^+ + HX$$

where $X = CH_3O^-$ or OH^-. In the route A, the reaction proceeds *via* the following mechanism.

$$2NHR_2 + CO_2 \rightleftharpoons (NH_2R_2)(O_2CNR_2) \qquad (3)$$

$$M(L)(ClO_4)_2 + (NH_2R_2)(O_2CNR_2) \longrightarrow M(L)(O_2CNR_2)(ClO_4) + NH_2R_2ClO_4 \qquad (4)$$

In the case of TMC complexes, carbamato complexes were obtained easily and cleanly *via* route (B), from the corresponding hydrogencarbonato ($X = OH^-$) or monomethylcarbonato complexes ($X = CH_3O^-$). The formation may occur *via* the following scheme.

$$M(L)(O_2CX)^+ \longrightarrow M(L)^{2+} + CO_2 + X^- \qquad (5)$$

$$M(L)^{2+} + CO_2 + X^- + NHR_2 \longrightarrow M(L)(O_2CNR_2)^+ + XH \qquad (6)$$

The $R_2NCO_2^-$ complexes thus obtained are listed in Table I.

As to the preparation of Ni(*rac*-Me$_6$[14]aneN$_4$)$(O_2CNR_2)^+$, it may be worth while to point out the following facts. The complex, Ni(*rac*-Me$_6$[14]aneN$_4$)$^{2+}$, is known to exist as isomeric α-, β-, and γ-forms.[5] Their N-H orientations are (up-down-up-down), (up-up-up-up), and (up-up-down-down) in terms of Bosnich's notation.[6] Of these three isomers, only the α-isomer reacts readily with a bidentate ligand such as oxalate, acetate, acetylacetonate, or tartrate to form cis-type six-coordinate complexes with the macrocyclic ligand folded. The thermodynamically most stable isomer is of the β-type, and the α-isomer isomerizes in neutral, or at much faster rate in basic media, to the β-isomer. Therefore, it is necessary to add dialkylamine after CO_2 is bubbled thoroughly into the solution containing α-Ni(*rac*-Me$_6$[14]aneN$_4$)$(ClO_4)_2$, when the carbamato complex is synthesized through route (A).

2.3 Structural Aspects

In order to investigate the influence of structural factors upon the efficient CO_2 uptake and to determine the coordination stereochemistries, single crystal X-ray analyses have been carried out on eight such compounds. IR and NMR spectral

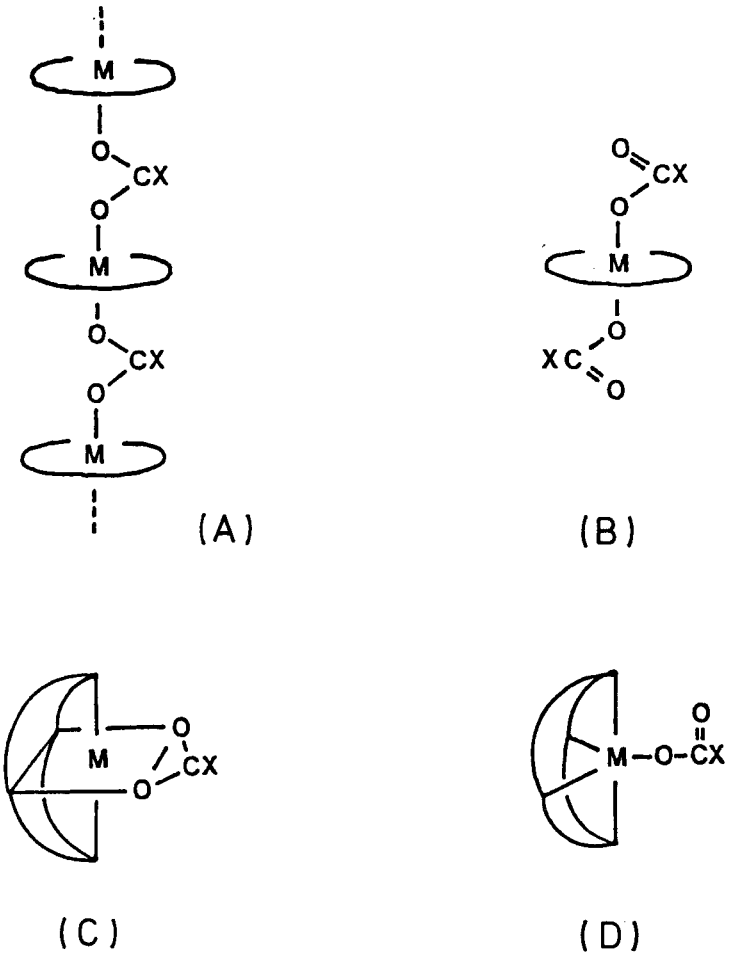

FIGURE 1 Structural types of M-(O_2CX) Complexes.

data on M-O_2CX complexes suggest that there are several coordination modes of the XCO_2^- ligand. The results of the X-ray analyses show that the M(L)(O_2CX) complexes are classified structurally into four groups, A-D (Figure 1).

In the type A structure, a metal ion is surrounded octahedrally, and bridge coordination of the XCO_2^- ligand forms a linear chain structure. A characteristic of this type of structure is very low solubility, and hence the compounds are easily isolated. The type A structure has been found X-ray crystallographically for [Zn([14]aneN$_4$)(O_2COCH_3)](ClO_4) (Fig. 2(a)), which is formed upon spontaneous CO_2 uptake from the air.

The type B structure was found for [Ni(Me_4[14]aneN$_4$)(O_2COCH_3)$_2$] (Fig. 2(b)). It is a discrete compound which does not exist as a linear chain. This compound is unstable in the solid state in the air and liberates CO_2 easily. Accordingly, the X-ray analysis of [Ni(Me_4[14]aneN$_4$)(O_2COCH_3)$_2$] was carried out at −105 °C.

In the structure C, the XCO_2^- ligand is chelated through two oxygen atoms to give a discrete cis-folded six-coordinate complex. This structure was found for

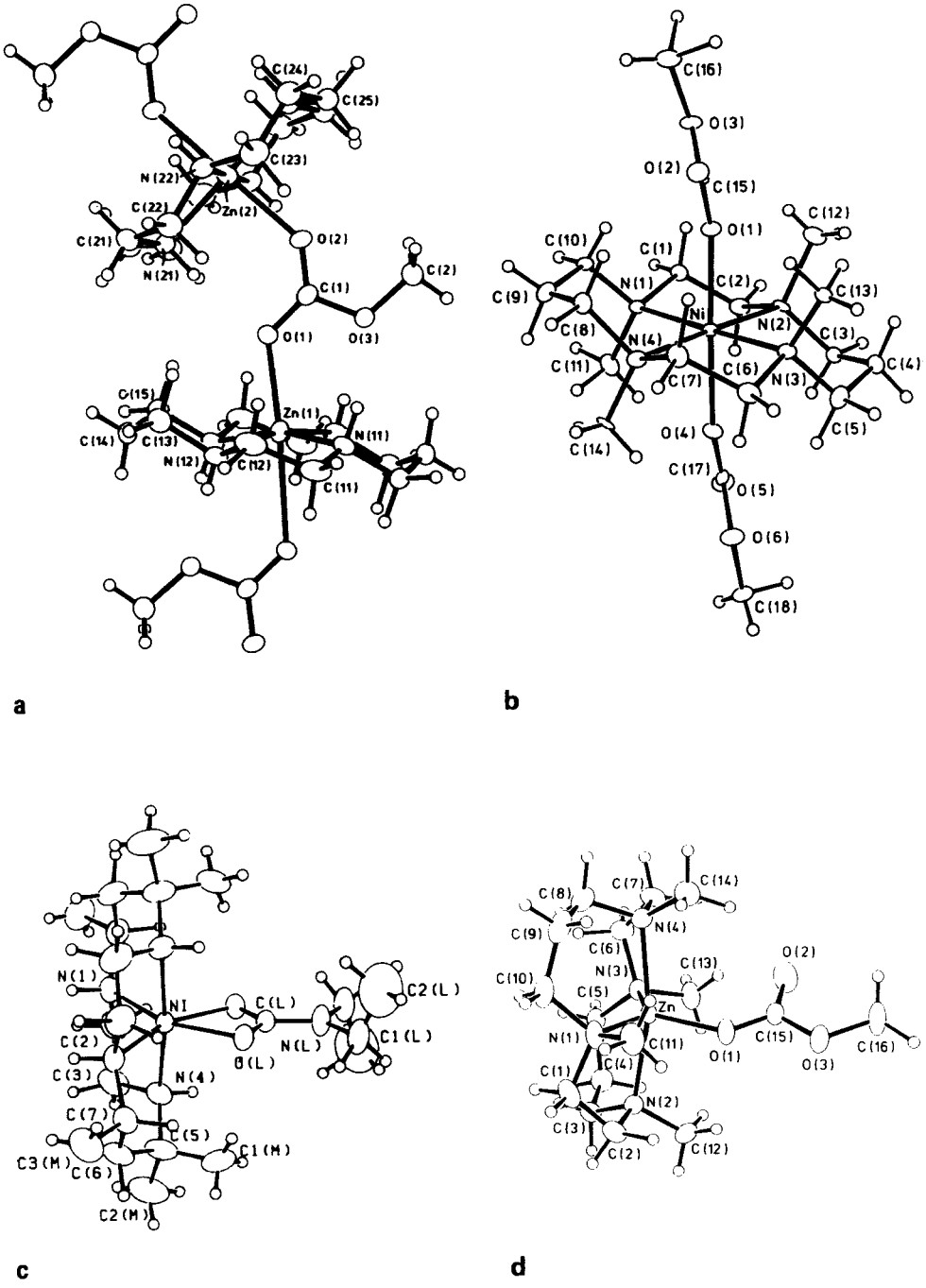

FIGURE 2 Examples of the structural types of M-(O_2CX^-) complexes: (a). $[Zn([14]aneN_4)(O_2COCH_3)]^+$. (b). $[Ni(Me_4[14]aneN_4)(O_2COCH_3)_2]$ (c). $[Ni(rac\text{-}Me_6[14]aneN_4)(O_2CNEt_2)]^+$; (d). $[Zn(Me_4[14]aneN_4)(O_2COCH_3)]^+$

TABLE II
Structural type of $M(L)(O_2CX)^+$ (assigned with the aid of X-ray analyses, IR, and/or NMR spectral data)†

M	L	$ROCO_2^-$	$R_2NCO_2^-$	$HOCO_2^-$
	[14]aneN$_4$	A‡	—	—
	[15]aneN$_4$	A‡	O	—
Zn^{2+}	Me$_2$[14]aneN$_4$	A	—	—
	TMC	D‡	O	D
	iso-[14]aneN$_4$	O	—	—
	[14]aneN$_4$	A	O	C
	[15]aneN$_4$	A	O	—
Ni^{2+}	TMC	B‡, D‡	C	—
	CTH	O	C‡	C
	iso-[14]aneN$_4$	A	—	—
Cd^{2+}	TMC	C	C	C

† R = Me, Et, and (n-alkyl). TMC and CTH stand for Me$_4$[14]aneN$_4$ and *rac*-Me$_6$[14]aneN$_4$, respectively.
‡ X-ray structure available. O structural type unassigned.
— the preparations have not been tried yet.

$[Ni(rac\text{-}Me_6[14]aneN_4)(O_2COH)]^+$ (Fig. 2(c)) and $[Cd(Me_4[14]aneN_4)(O_2COH)]^+$. Tetraazacycloalkanes such as *rac*-Me$_6$[14]aneN$_4$ and Me$_4$[14]aneN$_4$, which can fold readily, form this type of compound.

The type D structure contains a trigonal bipyramidal coordination geometry and the XCO_2^- ligand is coordinated to the metal in a unidentate fashion. $[M(Me_4[14]aneN_4)(O_2COCH_3)](ClO_4)$ (M = Zn and Ni) were found to assume this structure (Fig. 2(d)). This type of compound shows ν_{CO} at higher frequencies than complexes with the other coordination modes. ^{13}C NMR resonances of carbonate carbons of the type D compounds are at higher field by ~1-2 ppm than those of complexes with two equivalent CO bonds.

Table II shows the structural assignments for the $M(O_2CX)(L)^+$ complexes, which were made on the basis of the X-ray analyses, and IR and NMR spectral data.

2.4 IMPORTANT FACTORS IN THE DESIGN OF THE CO_2 UPTAKE SYSTEMS. - ROLES OF METAL ION AND MACROCYCLIC LIGAND -

Efficiency of the uptake reaction of XCO_2^- by ML^{2+} depends strongly on the system. Choice of metal ion and/or macrocyclic ligand, and possible coordination geometries about the central metal atom are particularly important. These are closely related to each other and cannot be discussed separately.

First of all, in order to allow the reaction to proceed successfully, the central metal ion must have coordination behavior such that it can form not only square-planar four coordiante complexes but also five- or six-coordinate complexes. Coordination of tetraazacycloalkane (L) leaves the metal ion coordinately unsatured. That is, the resulting ML complex has potentially vacant coordination sites where the uptake reaction takes place. To set up such a situation, use of tetradentate macrocycles is pertinent. As far as we tried, tetradentate macrocycles were much better than linear tetraamines such as trien or 3,2,3-tet. This is consistent with the fact that linear tetraamines are flexible, whereas macrocycles could bring about more rigid coordination geometries favorable to the uptake of XCO_2^-.

The cavity size of the tetraazacycloalkanes is also an important factor. For example, an analogous Zn^{2+} complex containing a similar tetraazacycloalkane with a larger cavity size ([16]aneN$_4$) does not give the desired monoalkylcarbonato complexes under the same conditions. Possibly a natural cavity size of [16]aneN$_4$ is somewhat larger than necessary to surround Zn^{2+} in a planar fashion, and thereby the resulting Zn([16]aneN$_4$) complex has a distorted tetrahedral coordination geometry. A Zn^{2+} complex having tetrahedral geometry is so stable that it would not undergo the further ligand uptake.

Tendencies of the macrocycle toward folding or toward square-planar coordination are also important. For example, the carbamato complexes M(L)$(O_2CNR_2)^+$ are formed only with Me$_4$[14]aneN$_4$ or *rac*-Me$_6$[14]aneN$_4$ which folds readily.

As to the efficiency of the isolation of M(L)$(O_2CX)^+$, the linear chain structure (type A) surpasses the other structural types because of the low solubility.

Zn^{2+}, Ni^{2+}, and Cd^{2+} with certain tetraazacycloalkanes fulfill the requirements and work nicely. Among the metal ions studied, Zn^{2+} is superior as to the efficiency. The square-planar Zn^{2+} complex is rare and, to our knowledge, its reactivity has not been studied. It seems that Zn^{2+} in such a circumstance tends strongly to take up additional ligands to give a five- or six-coordinate complex. This could be the driving force for the effective CO_2 uptake by the Zn^{2+} complexes.

2.5 SOLUTION BEHAVIOR OF ZN-O_2COR COMPLEXES

2.5.1 Reversible Absorption and Desorption of CO_2

^{1}H and ^{13}C NMR spectral studies show that the monoalkylcarbonato Zn^{2+} complexes, Zn-O_2COR, exist in organic solvents such as chloroform and dichloromethane in equilibrium with their decarboxylated Zn-OR complexes (Eq. (7)). The equilibrium involves reversible desorption and absorption of CO_2.

$$\text{Zn(L)–O}_2\text{COR} \rightleftharpoons \text{Zn(L)–OR} + \text{CO}_2 \qquad (7)$$

Identification of species in solution and NMR signal assignments were made with the aid of isotopically labeled $[Zn(L)(O_2{}^{13}COCH_3)](ClO_4)$ and $[Zn(L)(O_2CO{}^{13}CH_3)](ClO_4)$ derived from $^{13}CO_2$ and $^{13}CH_3OH$, respectively. As an example, ^{1}H NMR spectra of the $[Zn([15]aneN_4)(O_2COCH_3)](ClO_4)$ in $CDCl_3$ are shown in Fig. 3 ($^3J(^{13}CH) = 3.7$ Hz, $^1J\,^{13}CH = 141$ Hz for Zn-$O_2CO^{13}CH_3$, $^1J^{13}CH = 145$ Hz for Zn-$O^{13}CH_3$).

The equilibrium of Eq. (7) was studied in a sealed NMR tube by monitoring signal intensities of ^{1}H and ^{13}C resonances as a function of temperature. A decrease in temperature makes the equilibrium shift toward an increase in the amount of the Zn-O_2COCH_3 complex. The spectral changes were completely reversible in the range of $-40°C \sim +60°C$. Thus, CO_2 is absorbed and desorbed reversibly. The equilibrium constants ($K = [ZnO_2COR]/[ZnOR][CO_2]$) were determined to be $K_{60.4°C} = 2.2$, $K_{20.3°C} = 5.8$, $K_{0.4°C} = 12$ and $K_{-40.3°C} = 49$ M^{-1} (M = mol dm^{-3}). The thermodynamic parameters, ΔH and ΔS, were found to be -27 kJ mol^{-1} and -76 J K^{-1} mol^{-1}, respectively. The concentration ratio of ($[Zn\text{-}O_2COCH_3]/[Zn\text{-}OCH_3]$) at 0.4 °C is 2.3.

2.5.2 Conversion of the coordinated $ROCO_2^-$ ligand into dialkyl carbonate The monoalkylcarbonato ligands $R^1OCO_2^-$ of the Zn^{2+} complexes were successfully

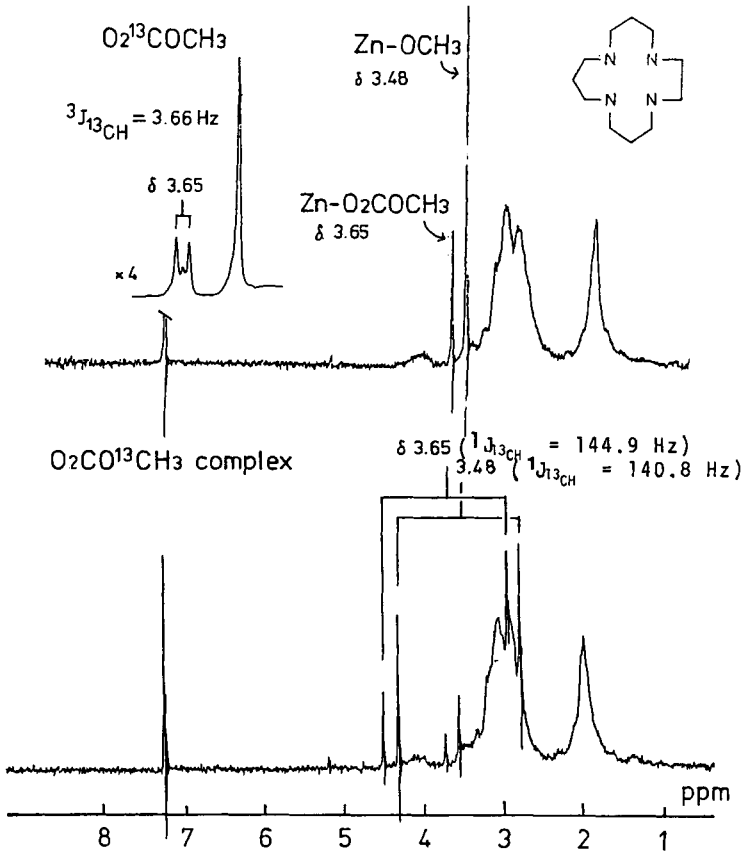

FIGURE 3 ^1H NMR spectra of $Zn([15]aneN_4)(O_2COCH_3)(ClO_4)$ and its ^{13}C labelled derivatives in $CDCl_3$.

converted into dialkylcarbonate, R^1OCOR^2, by treating with FSO_3R^2 (Scheme II). The alkylation of $R^1OCO_2^-$ was followed with ^1H NMR. When a small excess of FSO_3CH_3 was added to a $CDCl_3$ solution of $Zn(O_2COCH_3)([15]aneN_4)(ClO_4)$, the methyl proton singlet of $Zn\text{-}O_2COCH_3$ at $\delta = 3.65$ decreased gradually and a new singlet appeared at $\delta = 3.80$, the chemical shift of which was exactly the same as that of authentic dimethyl carbonate. After 24 hr, the signal at $\delta = 3.65$

Scheme II

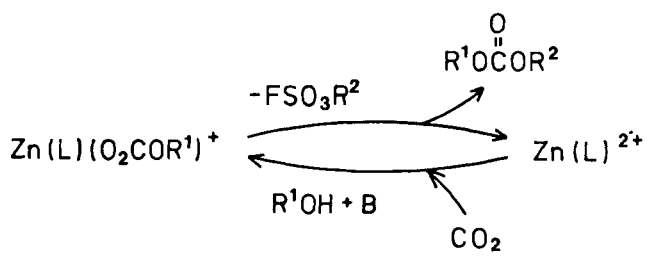

disappeared completely and the peak at $\delta = 3.80$ became much stronger. The formation of dimethylcarbonate was also confirmed by GC-mass spectral analysis. The zinc complex which had released monomethylcarbonato ligand reacted again with CO_2 in CH_3OH to give $Zn(O_2COCH_3)([15]aneN_4)(ClO_4)$, as shown in Scheme II. A series of Ni(II)-O_2COR complexes also undergo similar reaction to give the dialkylcarbonates.

3. CORRELATION BETWEEN AXIAL AND IN-PLANE COORDINATION BOND LENGTHS IN TETRAGONAL SIX-COORDINATE COMPLEXES OF THE *TRANS*-$[MX_2N_4]$ TYPE (M = Co^{3+}, Ni^{2+}, AND Zn^{2+}). X-RAY STRUCTURAL AND *AB INITIO* MO STUDIES

3.1 Introduction

Earlier studies of tetragonally distorted octahedral metal complexes suggest that, in complexes of this type, there exists an interaction between in-plane and out-of plane ligands through the metal ion.[7] Hathaway[8] and Gazo[7] demonstrated, on the basis of available X-ray data of metal ion salts and simple coordination compounds, correlations between in-plane and out-of-plane coordination bond lengths for some Cu^{2+} and Ni^{2+} complexes of this type. Generally, the in-plane bond distances increase as the out-of-plane distances decrease. Similar phenomena arising possibly from the same electronic origin have been reported for tetragonal metal complexes of this type. It has been noted, in the solution chemistry of some Co^{3+} complexes of this type, that equatorial ligands affect rates of hydrolyses of the axial ligands.[9] In an NMR spectral study of five-coordinate Cd^{2+} porphyrin complexes with substituted pyridines at the axial position, coupling constant between ^{111}Cd and porphyrin nitrogen (^{15}N) has been found to decrease with an increase in basicity of the substituted pyridine.[10] Busch and coworkers observed a similar phenomenon in ligand field electronic spectra.[11] They showed that, in Ni^{2+} complexes of trans-NiX_2N_4 type, ligand field strength of an axial ligand (Dq^z) decreases as an in-plane ligand field (Dq^{xy}) increases, and they termed it the "electronic cis effect".[11] It has been also shown on the Ni^{2+} complexes that the electronic cis effect is manifested in far infrared spectra due to coordination bond stretch vibrations.[14]

The occurrence of such an interaction between in-plane and out-of-plane ligands through a metal ion, as well as the degree of the interaction, should be metal ion dependent. A series of the studies[12–14] was undertaken in order to investigate the electronic effect in a more systematic and quantitative way in order to elucidate the role and function of the metal ion in the observed phenomenon. We have carried out X-ray analyses and *ab initio* MO calculations[15] for a series of complexes which have the same or very similar coordination environments. As metal ions, we chose Co^{3+}, Ni^{2+}, and Zn^{2+} because of the following reasons:

i) these metal ions form tetragonal complexes of this type;

ii) routine application of an *ab initio* MO method is in hand in this laboratory for complexes of first row transition metal ions.

In the experimental approach, we have determined the structures of a series of complexes of *trans*-MX_2N_4 type, where X is halide or pseudo-halide ion. Tetraazacycloalkanes with different ring sizes, $[14]aneN_4$, $[15]aneN_4$, and $[16]aneN_4$, were mainly used as in-plane ligands so as to vary the M-N distance systematically. As axial ligands (X), we chose Cl^- and NCS^-, which have relatively weak and strong ligand field strengths, respectively, so that it is possible to

investigate the effect of ligand field strength on the correlation between M-X and M-N distances. In the theoretical approach, we have carried out ab initio MO calculations on model systems, *trans*-$MCl_2(NH_3)_4$ (M = Co^{3+}, Fe^{2+}, Ni^{2+}, and Zn^{2+}).[16] We discuss electronic factors, or metal ion characteristics, which bring about the experimentally observed correlation of intramolecular coordination bond lengths in terms of potential energy surfaces along M-N and M-Cl bond axes.

3.2 Correlation between Axial and In-plane Coordination Bond Lengths in trans-MX_2N_4 Type Complexes

Table III collates the average in-plane (M-N) and axial (M-X) coordination bond lengths of the complexes studied. As expected, with an increase in the number of ring members in macrocyclic ligands, the in-plane M-N distance increases. This increase amounts to 0.04-0.06Å for each ring member added. They are not as large as expected from calculations of strain energy minimizations for free ligand molecules (0.10-0.15Å).[17] Data reported previously for the same type of complexes with other similar tetraaza macrocyclic or diamine ligands are also included in Table III. The

TABLE III
Average in-plane and axial coordination bond lengths in complexes of *trans*-MX_2N_4 type[a]

Compounds	M-X/Å	M-N/Å	Ref. No.
$[NiCl_2([14]aneN_4)]$	2.5101(4)	2.067(1)	14,24
$[NiCl_2([15]aneN_4)]$	2.497(1)	2.114(10)	14
$[NiCl_2([16]aneN_4)]$	2.482(54)	2.171(34)	14
$[NiCl_2(N_47)]$[b]	2.548(8)	2.068(16)	19
$[NiCl_2(N_49)]$[c]	2.426(1)	2.161(75)	19
$[Ni(NCS)_2([14]aneN_4)]$[d]	2.130(2)	2.067(3)	14
	2.128(2)	2.071(5)	14
	2.108(2)	2.081(5)	14
	2.119(6)	2.078(6)	14
$[Ni(NCS)_2([15]aneN_4)]$	2.079(20)	2.131(25)	14
$[Ni(NCS)_2([16]aneN_4)]$	2.077(26)	2.179(32)	14
$[Ni(NCS)_2(NH_3)_4]$	2.07(3)	2.15(2)	25
$[Ni(NCS)_2(en)_2]$	2.15	2.10	26
$[Zn(NCS)_2([14]aneN_4)]$	2.367(25)[h]	2.104(25)	13
$[Zn(NCS)_2([15]aneN_4)]$	2.282(8)[h]	2.146(28)	13
$[CoCl_2([15]aneN_4)]$[e]	2.259(31)	2.001(56)	27
$[CoCl_2(en)_2]^+$	2.257(1)	1.955(4)	28
$[CoCl_2(tn)_2]^+$[f]	2.26	2.00	29
$[CoCl_2(cptn)_2]^+$[g]	2.258(3)	1.978(5)	30

[a] A number in parentheses is an esd for a mean value of more than two chemically or crystallographically inequivalent bond lengths and is equal to $[\Sigma\Delta_i^2/(n-1)]^{1/2}$, where Δ_i is the deviation of the i-the value i a set of n such values from arithmetic mean of the n values. In case of $n = 2$, it is taken to be the largest of three values: the esd for one parameter (q_1), the esd for the other (q_2), or $|q_1 - q_2|/2$.

[b] N_47 = 1,4,7,10-tetraazacyclotetradecane.

[c] N_49 = 1,4,7,10-tetraazacyclohexadecane.

[d] There are four crystallographically independent complexes in the unit cell.[14]

[e] Green form isomer.

[f] tn = 1,3-propanediamine.

[g] cptn = 1,2-cyclopentanediamine.

[h] An average value of Ct-NCS distances, where Ct denotes a center of the cavity formed with four in-plane nitrogens (see Ref. 13).

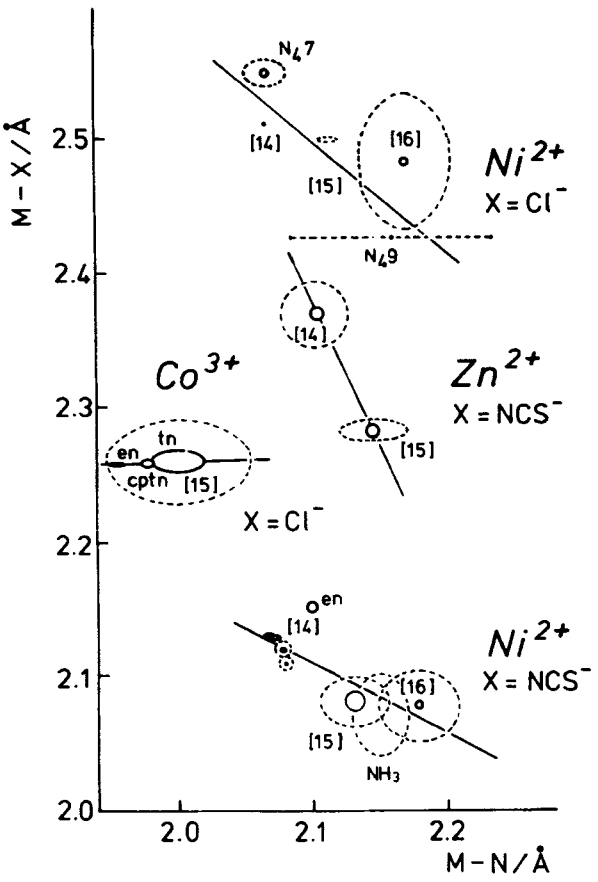

FIGURE 4 Correlation between axial and in-plane coordination bond lengths in complexes of the *trans*-MX_2N_4 type. Size of a dashed ellipse or line illustrate an esd obtained upon averaging chemically or crystallographically inequivalent distances, while that of a full-line figure within the dashed one shows an arithmetic mean of esd's for individual metal-ligand distances (see footnote a) in Table III). Ligand abbreviations: [14] = [14]aneN$_4$; [15] = [15]aneN$_4$; [16] = [16]aneN$_4$. See footnotes of Table III for others. For the en complex, no esd values were reported.

correlations are shown in Figure 4, in which the M-X distances are plotted on the vertical axis and the M-N distances on the horizontal one.

As is seen in Figure 4, there exists a negative correlation between M-X and M-N distances for complexes of each metal ion with given axial ligands: axial coordination bond length decreases as in-plane distance increases, generally. Although there exist steric effects in the molecular and crystal structures of the compounds that cause the large standard deviations in the average coordination bond lengths,[13,14] they are characteristic of each system and should not give rise to the correlation shown in Figure 4. Thus, the nature of the phenomenon must be electronic in origin.

In the crystal structure of *trans*-[Ni(NCS)$_2$([14]aneN$_4$)], there are four crystallographically nonequivalent molecules.[14] Interestingly, data for these four molecules show clearly a trend for the negative correlation within the very limited range of metal-ligand distances (see Figure 4).

Among the present three metal ions, the Zn^{2+} system shows the strongest correlation, the Co^{3+} system almost no correlation, and the Ni^{2+} system is intermediate.

When the $NiCl_2N_4$ and $Ni(NCS)_2N_4$ systems are compared, the slope for the chloro complexes is steeper than that for the isothiocyanato complexes. This indicates that the weaker the axial ligand field is, the stronger is the correlation (*vide infra*). It should be noted that the Zn^{2+} system has a steep slope in spite of the fact that the data have been obtained with complexes with strong axial ligands NCS^-.[18]

For the Ni^{2+} system, it is possible to observe changes in the M-N distances of complexes having the same in-plane ligand by altering the axial ligand. Although the number of data for such comparisons are very limited and the changes in the M-N distances are very small, it is likely that there exist negative correlations between M-X and M-N distances in each of $[NiX_2([14]aneN_4)]$, $[NiX_2([15]aneN_4)]$, and $[NiX_2([16]aneN_4)]$.

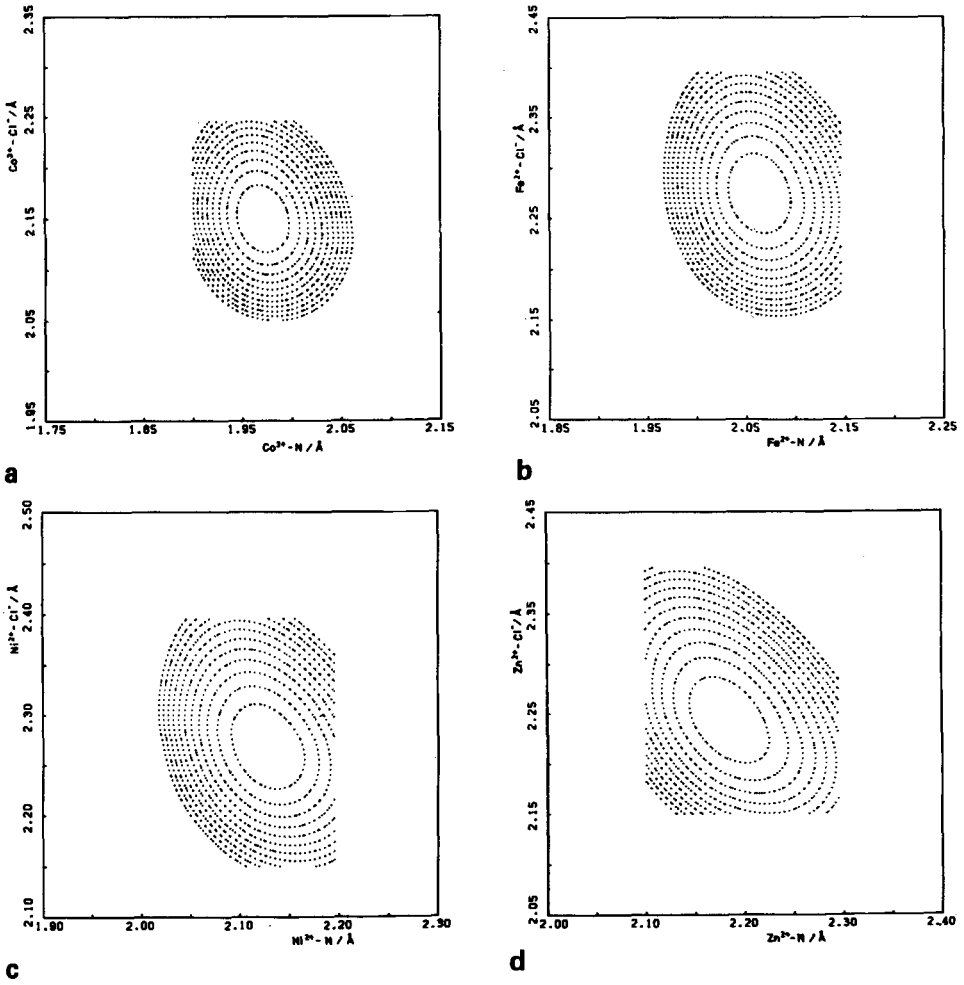

FIGURE 5 Potential energy surfaces of *trans*-$[MCl_2(NH_3)_4]$ along the M-Cl (vertical axis) and M-N (horizontal axis) coordination bonds: (a) *trans*-$[CoCl_2(NH_3)_4]^+$; (b) *trans*-$[FeCl_2(NH_3)_4]$; (c) *trans*-$[NiCl_2(NH_3)_4]$; (d) *trans*-$[ZnCl_2(NH_3)_4]$. Contours are at intervals of 0.5 kcal mol^{-1}.

Coordination geometries found for Ni^{2+} complexes with the $N_4$7 ligand may provide further evidence for the occurrence of such an electronic cis effect. The structures of $[NiCl_2(N_4 7)]$[19] and $[Ni(NCS)_2(N_4 7)]$[20] have been found to be of trans and cis types, respectively. It is most reasonable to consider the observed cis and trans stereochemistries to be a result of the electronically controlled cis effect in view of the relative size between the cavity of the $N_4$7 ligand and a high spin octahedral Ni^{2+}, and the relative ligand field strength between Cl^- and NCS^- ligands.[14,20]

3.3 Potential Energy Surfaces of trans-$[MCl_2(NH_3)_4]$ ($M = Co^{3+}$, Fe^{2+}, Ni^{2+}, and Zn^{2+}) along Coordination Bond Axes

Figure 5 shows the calculated potential energy surfaces for the Co^{3+}, Fe^{2+}, Ni^{2+}, and Zn^{2+} complexes, M-Cl distances being plotted on the vertical axis and M-N distances horizontally. The MO calculations for a hypothetical low spin Fe^{2+} complex, trans-$[FeCl_2(NH_3)_4]$, have been carried out in order to investigate the effect of electric charge, since experimental data have been obtained with complexes of divalent metal ions except for the Co^{3+} system. The Fe^{2+} complex is isoelectronic with the Co^{3+} complex and its ground state was assumed to be closed-shell singlet.

The calculated maps of the potential surfaces have the following common features:

i) each contour is an ellipse elongated in the M-Cl direction;

ii) each ellipse has an anticlockwise tilt.

When the maps shown in Figure 5 are compared, the ellipse for Co^{3+} is the closest to a circle, the axis ratio of the Zn^{2+} ellipse is the largest, and the Ni^{2+} system is intermediate. The tilt of the ellipse is the smallest for Co^{3+}, intermediate for Ni^{2+}, and the largest for Zn^{2+}. Contour lines are the most congested for Co^{3+}, while they are the farthest apart for Zn^{2+}. These features are very important in the interpretation of the experimentally observed correlation between the axial and in-plane coordination bond distances.

On the basis of the section map, we will discuss the case where the M-N distance is varied, as was done experimentally by use of the macrocyclic ligands with different ring sizes. When energy minimum points at various M-N distances are connected, a line with a slope (α) is obtained. This line shows the interrelationship between the M-Cl and M-N distances under the electronically most stable circumstances. Thus, the larger the

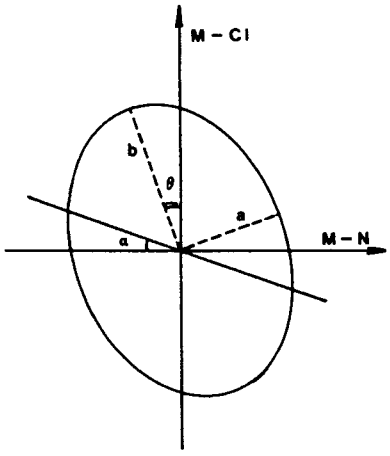

slope (α), the stronger the correlation. Assuming that each contour is a perfect ellipse, α is given by the following equation,

$$\tan^{-1}\alpha = [\{1-(a/b)^2\}\sin\theta\cos\theta]/[\sin^2\theta + (a/b)^2\cos^2\theta] \quad (8)$$

where θ denotes a tilt of the ellipse and a/b represents an axis ratio of the ellipse (b> a). As is clear from Eq. (8), it the contour is not an ellipse but a circle (a= b), or if the longer axis of the ellipse is parallel to the vertical axis ($\theta = 0$), α equals zero. Under such circumstances, the M-Cl distance does not change at all, even though the M-N distance is varied. The larger α value would be expected when the ellipse has a larger tilt[21] and the axis ratio of the ellipse is smaller.[22]

As the difference in the ligand field strengths between axial and in-plane ligands becomes larger, the ellipticity (a/b) decreases to give larger α. This is exemplified by the difference in the slopes for the chloro and isothiocyanato Ni^{2+} complexes, shown in Figure 4 (*vide supra*). In the present systems, the ellipse becomes more nearly circular with an increase in the axial ligand field strength. The closer the ellipse is to a circle, the weaker is the correlation. The Co^{3+} system demonstrates such a situation (see Figure 4 and Figure 5(a)).

The tilt of the ellipse in Figure 5 is 14° for Co^{3+}, 18° for Fe^{2+}, 30° for Ni^{2+}, and 41 for Zn^{2+}. The tilt reflects the ease with which electrons move when the coordination bond lengths are varied. Thus, it seems that the tilt is associated with polarizability of the complex. Generally, the M-Cl overlap population increases as the M-N distance increases. This arises from the fact that each metal atom tends to keep the electric charge neutral. In fact, within the computed range of M-N and M-Cl distances (the optimized distance ± 0.25Å), total electron population on the metal atoms (Mulliken population) was constant within 2% for each metal atom. The values were 26.4 for Co^{3+}, 25.5 for Fe^{2+}, 27.5 for Ni^{2+}, and 29.4 for Zn^{2+}. The dependence of the M-Cl overlap population upon the M-N distance is strongly metal ion dependent, and is closely related to the tilts of the ellipses of Figure 5.

The congestion of the contour lines, i.e., the slope of the potential surface, is also an important factor. If contour lines were less congested, the electronic cis effect would occur more easily. On the other hand, coordination bond lengths would not vary widely if the slope of the potential surface was steep. It is manifested in the Co^{3+} system (see Fig. 4 and Fig. 5(a)). The most apparent difference in the feature of the potential surfaces between the Co^{3+} and Fe^{2+} complexes is the slopes. There is no doubt that the Co^{3+} surface becomes steeper by the effect of the electric charge. Higher electric charge on the metal brings about more congested contour lines.

The conclusions obtained from the features of the potential surfaces, such as the axis ratio and tilt of the ellipse and the degree of the congestion of the contour lines, agree very well with the experimentally observed results shown in Figure 4.

Pearson made the following statement in his paper describing the concept of Hard and Soft Acids and Bases: Softness in both the acid and base means that the repulsive part of the potential energy curve rises less sharply than for hard acids and bases.[23] According to this, it follows that the degree of the congestion of the contour lines in Figure 5 shows the hardness of the metal ions. Furthermore, softness (or hardness) is known to be directly associated with the polarizability,[23] which is correlated with the tilt of the ellipse in Figure 5. In view of these considerations, it is clear from Figures 4 and 5 that, among the metal ions studied, Co^{3+} is the hardest, Zn^{2+} is the softest, and Ni^{2+} is intermediate. Although Pearson classifies both of Ni^{2+} and Zn^{2+} into borderline Lewis acids,[23] there is a clear difference in softness between them.

Both theoretically and experimentally, it has been found that the degree of correlation increases in the order, $Co^{3+} < Ni^{2+} < Zn^{2+}$. It should be pointed out that the number of d-electrons in the e_g orbital in O_h symmetry increases in the same order: 0 for Co^{3+}, 2 for Ni^{2+}, and 4 for Zn^{2+}.

4 STABILIZATION OF HIGH OXIDATION STATES OF METAL IONS AND ITS APPLICATION TO CHEMISTRY OF ONE-DIMENSIONAL HALOGEN-BRIDGED M^{2+}-M^{4+} MIXED-VALENCE COMPLEXES

4.1 Introduction

Metal ions with unusually high oxidation states impart interesting physical, bioinorganic and redox properties, and much attention has been paid to these aspects.[31–33] However frequenctly these high oxidation states are not stable enough to be isolated. The incorporation of a metal ion into a macrocyclic framework affords possible access to unusually high oxidation states. Trapping the highly oxidized metal cation in a framework reduces the tendency of the cation to react with the solvent or with the substances dissolved in the solution and makes the unusually high oxidation states sufficiently stable. This is evidenced by the fact that Ni^{2+} and Cu^{2+} complexes of neutral macrocyclic ligands undergo one "reversible or nearly reversible" oxidation process in acetonitrile to give Ni^{3+} and Cu^{3+} species.[34–38]

The exceptionally strong ligand field exerted by a macrocyclic ligand is another factor that makes high oxidation species easily obtained. Antibonding levels in the species of lower oxidation state are raised to such high energy that electrons are easily removed.[38–41] Many Ni^{3+} and Ag^{2+} complexes and otherwise unstable Ag^{3+} and Cu^{3+} complexes with macrocyclic ligands have become now familiar in coordination chemistry.[31–34,38,42]

4.2 Ni^{3+}, and Ag^{2+} Complexes

The remarkable ability of certain tetradentate cyclic amines to stabilize unusual oxidation states of transition metals was demonstrated by the preparation and isolation of Ni^{+} and Ni^{3+} complexes.[35] The relative stability of Ni^{3+} complexes can be expressed by the half-wave potential of the Ni^{2+}/Ni^{3+} couple. The redox behavior is a function of degree and type of ligand unsaturation, ring size of the macrocycles, number and position of ring substituents, charge type, coordination number, and the anion X in $Ni^{III}X_2L$.[36,40,43–48]

A series of $[NiX_2L]ClO_4$ (L = [13]aneN$_4$, [14]aneN$_4$, [15]aneN$_4$, Me$_2$[14]aneN$_4$, and *meso*-Me$_6$[14]aneN$_4$) have been prepared and characterized.[49–52] The effective magnetic moments of the Ni^{3+} complexes at room temperature are ~1.8 - 2.0 BM corresponding to one unpaired electron. Electron spin resonance studies provide evidence for the electron density distribution.[36,49,52,53] It gives information about the distinction between authentic d^7 Ni^{3+} complexes and Ni^{2+}-stabilized ligand radicals. For authentic Ni^{3+} complexes with tetragonal symmetries, anisotropic EPR spectra of axial symmetry with $g_{\parallel} > g_{\perp}$ and superhyperfine splitting of the $g_{\parallel}$ feature were observed. They are consistent to low-spin d^7 configuration with an unpaired electron occupying principally d_{z^2} orbital.

The crystal structures of the complexes, $[NiCl_2([14]aneN_4)]ClO_4$,[54] $[Ni(NCS)_2([14]aneN_4)]ClO_4$,[55], and $[Ni(H_2(H_2PO_4)_2(meso\text{-}Me_6[14]aneN_4)]$,[48] have been determined. Ni ions are octahedrally surrounded by a square-planar array of four nitrogens of the macrocycles and by two X ions occupying the axial positions. The average Ni^{III}-N distances are 1.970 - 1.973 Å, and they are significantly shorter than the values of the corresponding Ni^{2+} complexes.[14,24]

Ag^{2+} and Ag^{3+} ions are rather unstable due to the powerful oxidizing nature of these ions in solution.[34] But these unfamiliar oxidation states of silver are strongly stabilized by coordination with nitrogen-containing heterocycles such as pyridines, polypyridines and macrocycles. Tetraaza macrocyclic complexes of Ag^{2+}were obtained from solution

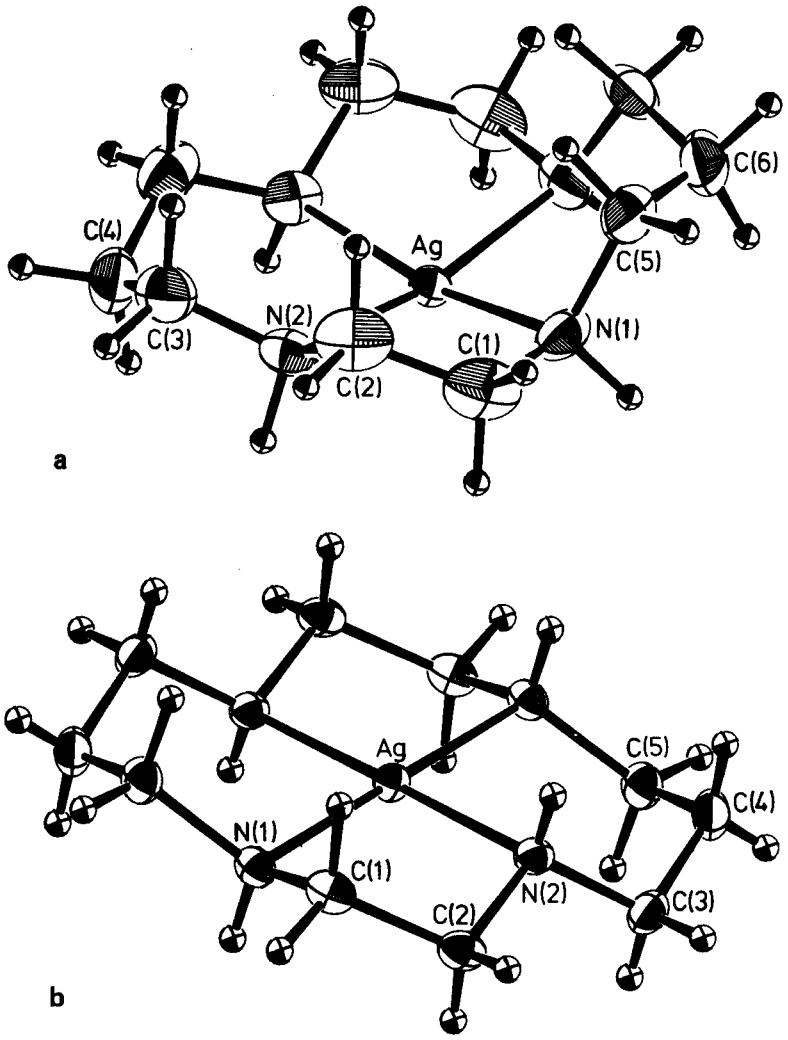

FIGURE 6 Perspective views of two isomers of $[Ag([14]aneN_4)]^+$; (a), red-orange needle (Pbnm); (b), yellow block ($P\bar{1}$).

containing Ag^+ salts and macrocyclic tetramines through the following disproportionation reaction.[56,57]

$$2Ag^+ + L \longrightarrow AgL^{2+} + Ag^0 \qquad (9)$$

They are exceptionally stable in most solvents in which they are soluble (e.g., acetonitrile, water, ethanol). Some of these Ag^{2+} species have been oxidized both chemically and electrochemically to Ag^{3+} species of substantial stability.[57]

X-ray crystallographic studies[58,59] revealed that the Ag^{2+} complexes are square planar, or distorted octahedral with weak interaction on axial positions due to strong Jahn-Teller effect for d^9 system.

Two isomers of $[Ag([14]aneN_4)](ClO_4)_2$, red-orange needles and yellow blocks have been isolated.[59] The red-orange needles decompose slowly to unknown products in dilute acid, but isomerize to yellow blocks in alkaline solution (pH = 10). The yellow isomer is stable in water or in dilute acid. In their X-ray structures, the silver atoms are surrounded by a square planar array of four nitrogen atoms (Fig. 6).

In the needle crystal, no axial interaction was found and the silver atom is located 0.23Å below the N_4-plane (the basket type conformation). On the other hand, in the yellow blocks, the silver is located at a crystallographic center of symmetry and therefore exactly in the N_4-plane (the cyclam type). A weak axial interaction with one of the perchlorate oxygens is observed (Ag-O = 2.788(2)Å). The average Ag-N distances are 2.192(11) and 2.158(2)Å for the basket and the cyclam type structures, respectively. The bond distances of the $[Ag(meso\text{-}Me_5[14]aneN_4](NO_3)_2$ in which Ag sits on the center of symmetry are 2.160(3)Å for Ag-N and 2.807(4)Å for Ag-O.[58]

The basket type conformation may be preferable for such disproportionation reaction, and the red-orange form can be taken as a kinetic isomer. It isomerizes in basic solution to the thermodynamically more stable yellow isomer (thermodynamic isomer) in which $[14]aneN_4$ takes the most stable ligand conformation. For metals with smaller ionic size, such as the first transition metals, the cyclam-type complexes are familiar. For larger ions such as Hg^{2+},[60] the basket type structure is preferred. Since the radius of Ag^{2+} (0.89Å) is intermediate, isomers of both types were isolated.

EPR spectra of the Ag^{2+} complexes are typical of a d^9 axial system. In each case $g_{\parallel}$ and $g_{\perp}$ are well resolved. This is expected for a planar d^9 complex.[59,60] EPR spectra of the needles and blocks in frozen 0.01 M $HClO_4$ solutions at 77 K were very similar to each other and exhibit axial symmetry.

4.3 *M^{2+}-M^{4+} Mixed Valence Complexes of Pd and Ni*

One-dimensional M^{2+}-M^{4+} mixed valence complexes of Pt and Pd have attracted much interest from the viewpoint of the chemistry and physics of low-dimensional compounds.[61-67] In compounds of this class, square-planar four-coordinate M^{2+} and trans-dihalogeno octahedral M^{4+} are stacked alternately in the direction of the needle axis, constructing halogen-bridged linear chains of $\cdots$X-M^{4+}-X$\cdots$ $M^{2+}\cdots$ segments, as shown below.

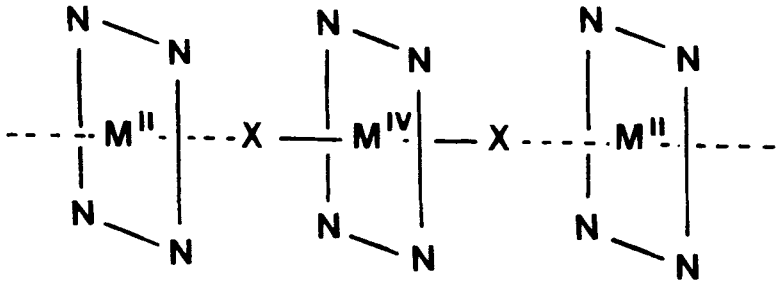

They show characteristic properties such as metallic luster, remarkable dichroism, and semiconducting nature arising from the electronic interaction between M^{2+} and M^{4+} through the bridging halogen atom.

Recently, this class of compounds have attracted much interest in the field of solid state physics and chemistry, since the bond alternation in this chain can be taken as Peierls distortion — a sort of the Jahn-Teller effect — and the one dimensional structure can be a good model for the Peierls-Hubbard theory in which an electron-phonon interaction is taken into account.

In compounds of this type, a ratio between M^{4+}-X and $M^{2+}\cdots X$ distances is correlated strongly to physical properties along the chain.[68] As the ratio approaches to unity, the difference between the oxidation states of M^{2+} and M^{4+} decreases, and the two metal are becoming equivalent to be tervalent. Under such extreme conditions, the compound should show metallic behavior.

Information about the intervalence interaction is obtained from electronic spectra, from electrical conductivities, from X-ray photoelectron spectra (XPS), etc. The energies of intervalence charge transfer band are lower, and electrical conductivities are higher, as the intervalence interactions are stronger. The interactions depend on the kind of metal, bridging halogens, counter anions, and in-plane ligands.

So far, many studies have been carried out on Pt complexes but fewer on Pd and Ni compounds, since the M^{4+} states of the latter are less stable. We have prepared and characterized M^{2+}-M^{4+} mixed valence complexes of Pd and Ni containing tetraazacycloalkanes or linear tetramines.[69-71]

There are two routes for the synthesis of the Pd^{2+}-Pd^{4+} mixed valence complexes, which are shown in Scheme III.

Scheme III

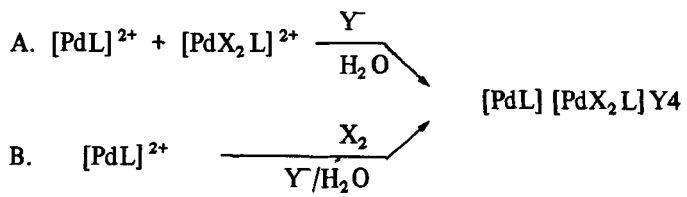

L = [14]aneN$_4$ and [15]aneN$_4$

X = Cl^- and Br^-

Y = ClO_4^- and PF_6^-

These compounds have been characterized by means of elemental analyses, electronic spectra (Nujol mull, $\tilde{\nu}_{max} \simeq 19000\ cm^{-1}$ for the Cl-bridged complexes and 12000 cm^{-1} for the Br-bridged complexes), electrical conductivities (pellet, $\sigma_{r.t.} \simeq 10^{-10}\ \Omega^{-1}\ cm^{-1}$ for the Cl-bridged complexes and $10^{-7} \sim 10^{-8}\ \Omega^{-1}\ cm^{-1}$ for the

TABLE IV
Averaged coordination bond distances (Å) and angles (°) with their esd's.

Compound	[PdL][PdCl$_2$L] (ClO$_4$)$_4$ (1)	[PdL][PdCl$_2$L] (PF$_6$)$_4$ (2)	[PdL](ClO$_4$)$_2$ (3)	[PdCl$_2$L](NO$_3$)$_2$ HNO$_3$ H$_2$O (4)
Pd^{4+}-Cl	2.319(3)	2.309(3)		2.303(1)
$Pd^{2+}\cdots$Cl	3.219(3)	3.514(3)		
$Pd^{2+}\cdots Pd^{4+}$	5.533(4)	5.819(2)		
Pd-N	2.055(5)	2.049(8)	2.051(7)	2.062(4)
Cl-Pd-N(1)	86.7(2)	87.0(1)		88.4(8)
Cl-Pd-N(2)	90.6(2)	90.1(2)		91.6(3)
N-Pd-N ($5^{\ddagger}$)†	84.9(2)	85.0(3)	83.0(3)	84.8(1)
Pd-N-C ($5^{\ddagger}$)	106.7(6)	106.9(6)	108.1(11)	106.8(1)
Pd-N-C ($6^{\ddagger}$)	115.6(5)	116.0(5)	115.8(6)	115.6(2)

† Abbreviations; $5^{\ddagger}$: 5-membered ring, $6^{\ddagger}$: 6-membered ring.

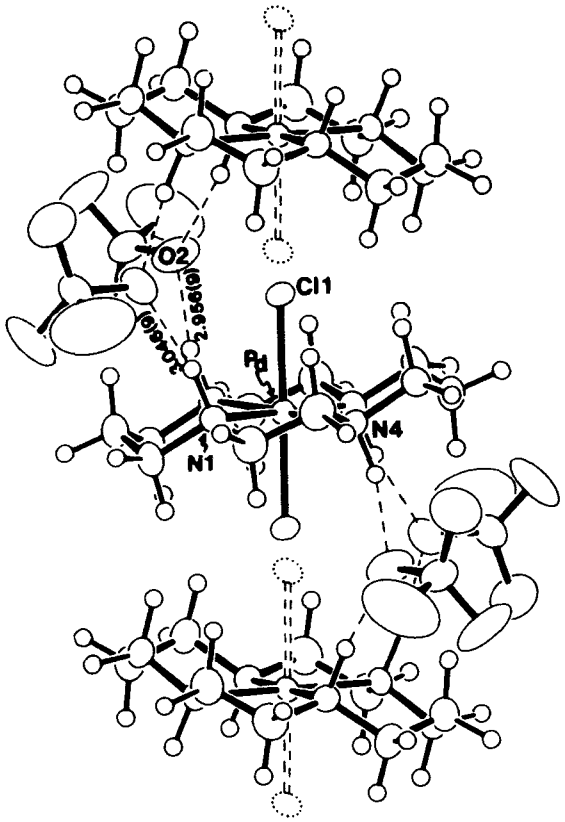

FIGURE 7 Perspective view of $[Pd([14]aneN_4)][PdCl_2([14]aneN_4)](ClO_4)_4$.

Br-bridged complexes), magnetic moments (diamagnetic), XPS, and X-ray analyses of the compounds, $[Pd^{II}([14]aneN_4)][Pd^{IV}Cl_2([14]aneN_4)]Y_4$ (Y = ClO_4^- (**1**)[69] and PF_6^- (**2**)[70]). All the data suggest that electronic interactions between Pd^{2+} and Pd^{4+} are stronger in the Br-bridged complexes than in the Cl-bridged ones.

The comparison of geometrical parameters of the chain structure with those of discrete Pd^{2+} and Pd^{4+} complexes provides unique information. To our knowledge, a study from such a standpoint has not been reported for this type of one-dimensional complex. We have determined X-ray structures of $[Pd^{II}([14]aneN_4)](ClO_4)_2$ (**3**), and $[Pd^{IV}CL_2([14]aneN_4)](NO_3)_2 \cdot (HNO_3) \cdot (H_2)$ (**4**) as well as **1** and **2**. Table IV collates the averaged coordination bond lengths and angles. In all these compounds, the in-plane ligands adopt the same (most stable) ring conformation. Figure 7 shows the structure of **1**.

The bridging Cl^- ions in the mixed valence complexes are statistically disordered, as has often been found in this type of complex. The disorder is brought about by a random arrangement among the chains. The similarities of Pd-N distances as well as the similarities of the geometrical arrangement of the in-plane ligand around Pd atom in Pd^{2+}, Pd^{4+}, and Pd^{2+}-Pd^{4+} complexes (Table IV) are responsible for this kind of disorder.

The Pd^{4+}-Cl^- distances in the mixed valence complexes are slightly elongated as compared with those of the discrete Pd^{4+} complex owing to electronic interactions along the chain direction.

Changing the counter anion from ClO_4^- to PF_6^- causes the separation of $Pd^{2+}\cdots Pd^{4+}$ or $Pd^{2+}\cdots Cl^-$ larger, depending on the size of anion connecting the neighbouring Pd^{2+} and Pd^{4+}. The ratios of Pd^{4+}-Cl^- to $Pd^{2+}\cdots Cl^-$ distance are 0.72 for **1** and 0.66 for **2**, respectively. The value indicate the electronic interaction along the chain is stronger in **1**. The same trend has been found in the electrical conductivities and electronic spectra.[71]

Similar one-dimensional Ni^{2+}-Ni^{4+} mixed valence complexes $[NiL][NiX_2L](ClO_4)_4$ (L = [13]aneN$_4$, [14]aneN$_4$, [15]aneN$_4$, 2,3,2-tet, and 3.2,3-tet; X = Cl^- and Br^-), have been synthesized by the following two methods.[62,71]

SCHEME IV

A: L = 2,3,2–tet and 3,2,3–tet

$$Ni(L)Cl_2 \xrightarrow[\text{abs. MeOH}]{Cl_2} [Ni^{III}Cl_2L]Cl \xrightarrow[70\%\ HClO_4]{} [NiL][NiCl_2L](ClO_4)_4$$

B: L = [13]aneN$_4$, [14]aneN$_4$, and [15]aneN$_4$

$$NiL(ClO_4)_2 \xrightarrow[70\%\ HClO_4]{Br_2} [NiL][NiBr_2L](ClO_4)_4$$

So far, the Cl-bridged complexes with tetraazamacrocycle have not been isolated since the more stable Ni^{3+} complexes are generally obtained under such preparative conditions.

They are formally tervalent, but are diamagnetic, black in color, and they have fairly large conductivities, as compared with Pt and Pd analogs. The electrical conductivities (pellet) at room temperature are on the order of $10^{-6}\ \Omega^{-1}\ cm^{-1}$ for the Br-bridged complexes and 10^{-7} - $10^{-8}\ \Omega^{-1}\ cm^{-1}$ for the Cl-bridged complexes.

The authenticity of Ni^{2+}-Ni^{4+} mixed valence states were directly evidenced by the XPS spectra (Table V).[71] In discrete complexes, the binding energy of $Ni2p_{3/2}$ depends strongly on the valence state of Ni and increases by *ca.* 1 eV as the oxidation number varies by + 1. In the linear chain compounds, $Ni2p_{3/2}$ values of Ni^{2+} and Ni^{4+} species are shifted toward the Ni^{3+} values. The difference in the binding energies between Ni^{2+}

TABLE V
Binding energy (eV) of some Ni^{2+}, Ni^{3+} and Ni^{2+}-Ni^{4+} mixed valence complexes

	$Ni2p_{3/2}$			Cl2p		
	Ni^{2+}	Ni^{3+}	Ni^{4+}	Cl^-		ClO_4^-
$[Ni([14]aneN_4)](ClO_4)_2$	855.1					207.6
$[NiBr_2([14]aneN_4)]ClO_4$		855.9				
$[NiCl_2([14]aneN_4)]ClO_4$		855.9			197.6[a]	20.75
$Ni(pn)_2Cl_3$	855.6		857.7	196.9[c]	198.4[b]	
$Ni([14]aneN_4)Br(ClO_4)_2$	855.2		856.9			207.9

[a] axial; [b] bridged; [c] counter ion.

TABLE VI

Average coordination bond distances of Ni^{2+}-Ni^{4+} mixed valence complexes and their reference compounds obtained from EXAFS and X-ray data

(A) Ni-N Bond:

Compound	r(EXAFS)	r(X-ray)	Δr
$[Ni(en)_2]SO_4$	2.14	2.124(6)	0.016
$[Ni[14]](ClO_4)_2$	1.94	1.945(8)	−0.005
$[NiCl_2[14]]$	2.09	2.067(1)	0.023
$[NiBr_2[14]]$	2.08	2.063(5)	0.017
$[NiCl_2[14]]ClO_4$	1.96	1.970(7)	−0.010
$[NiCl_2(en)_2]Cl$	1.96		
$[NiBr_2[14]]ClO_4$	1.95		
$[Ni(en)_2][NiCl_2(en)_2](ClO_4)_4$	1.92		
$[Ni(pn)_2][NiCl_2(pn)_2]Cl_4$	1.94		
$[Ni[14]][NiBr_2[14]](ClO_4)_4$	1.95		
$[Ni[15]][NiBr_2[15]](ClO_4)_4$	1.97		

(B) Ni-X Bond:

Compound	r(EXAFS)	r(X-ray)	Δr
$[NiCl_2[14]]$	2.50	2.510(1)	−0.010
$[NiCl_2[14]]ClO_4$	2.46	2.452(4)	0.008
$[NiCl_2(en)_2]Cl$	2.43		
$[Ni(en)_2][NiCl_2(en)_2](ClO_4)_4$	2.46		
$[Ni(pn)_2][NiCl_2(pn)_2]Cl_4$	2.46		
$[NiBr_2[14]]$		2.694(1)	
$[NiBr_2[14]]ClO_4$	2.62		
$[Ni[14]][NiBr_2[14]](ClO_4)_4$	2.69		
$[Ni[15]][NiBr_2[15]](ClO_4)_4$	2.59		
$[Ni(chxn)_2][NiBr_2(chxn)_2](BF_4)_4$	2.62		

and Ni^{4+} is smaller in the Br-bridged complex (1.7 eV) than in Cl-bridged complex (2.1 eV), indicating the stronger interaction in the former.

As to the Ni^{2+}-Ni^{4+} mixed valence complex, it is very difficult to grow single crystals suitable for X-ray analysis because Ni^{4+} state is unstable in solution. An EXAFS method has been applied to these compounds.[72] Coordination bond lengths about Ni^{2+} and Ni^{4+} have been successfully obtained (Table VI).

However, the contribution of the halogen atom X in the $Ni^{2+} \cdots X$ moiety to Ni-edge $Ni^{2+} \cdots X$ peak often overlaps with spectra due to $Ni \cdots C$ separations. Accordingly, it was difficult to determine full one-dimensional structural parameters from the EXAFS approach.

5. CONCLUDING REMARK

In this article, we presented three topics from our recent studies on the chemistry of tetraaza macrocyclic complexes. The content itself is not directly related to chemistry of macrocyclic compounds, but all of the chemistry described herein is accomplished by taking advantage, we believe in a sophisticated way, of the chemical and structural consequences of ligand macrocyclization. Our previous studies, "Sterically and electronically strained metal complexes — Complexes with medium sized chelate ring"[19,73], "Binuclear complexes with both metal ions bound within a large membered tetraaza macrocyclic ligand"[74], and "Unusually stable Al-C bond"[75], are also based on the utilization of chemical characteristics arising from the cyclic nature. Useful

molecular functions of synthetic macrocyclic compounds such as electrocatalyst[76] or novel oxidizing agent[77] have recently been reported. We hope that this article stimulates further research into new and important area of chemistry by making use of macrocyclic compounds.

REFERENCES

1. (a) R. Eisenberg and D.E. Hendriksen, *Adv. Catal.*, **28,** 79 (1979). (b) "Organic and Bioorganic Chemistry of Carbon Dioxide"; ed. by S. Inoue and N. Yamazaki, Kodansha, Tokyo, (1981).
2. For example: (a) J.C. Calabrese, T. Herskovitz, and J.B. Kinney, *J. Am. Chem. Soc.*, **105,** 5914 (1983). (b) S. Gambarotta, F. Arena, C. Floriani, and P.F. Zanazzi, *ibid.*, **104,** 5082 (1982). (c) M. Aresta and C.F. Nobile, *J. Chem. Soc., Chem. Commun.*, 636, (1975).
3. see (1a) and (1b) and references cited therein. The examples of the CO_2 insertion into the M-O bond are: (a) A.J. Goodsel and G. Blyholder, *J. Am. Chem. Soc.*, **94,** 6725 (1972). (b) M. Hidai, T. Hikita, and Y. Uchida, *Chem. Lett.*, 521 (1972). (c) T. Tsuda, S. Sanada, K. Ueda, and T. Saegusa, *Inorg. Chem.*, **15,** 2329 (1976). (d) M.H. Chisholm, F.A. Cotton, M.W. Extine, and W.W. Reichert, *J. Am. Chem. Soc.*, **100,** 1727 (1978). (e) T. Aida and S. Inoue, *ibid.*, **105,** 1304, (1983).
4. (a) M. Kato and T. Ito, *Inorg. Chem.*, **24,** 504 (1985). (b) M. Kato and T. Ito, *Inorg. Chem.*, **24,** 509 (1985). (c) H. Ito and T. Ito, *Bull. Chem. Soc. Jpn.*, **58,** 1755 (1985).
5. N.F. Curtis, D.A. Swann, and T.N. Waters, *J. Chem. Soc., Dalton*, 1063 (1973).
6. B. Bosnich, M.L. Tobe, and G.A. Webb, *Inorg. Chem.*, **4,** 1100 (1965).
7. J. Gazo, R. Boca, E. Jona, M. Kabesova, L. Macaskova, and J. Sima, *J. Coord. Chem. Rev.*, **43,** 87 (1982), and references cited therein.
8. B.J. Hathaway and A.A.G. Tomlinson, *Coord. Chem. Rev.*, **5,** 1 (1970).
9. J.F. Endicott and B. Durham, "Coordination Chemistry of Macrocyclic Compounds" ed by G.A. Melson, Plenum Press, New York, N.Y. (1979), Chap. 6.
10. D.D. Domoinguez, M.M. King and H.J. Yeh, *J. Mag. Reson.*, **32,** 161 (1978).
11. L.Y. Martin, C.R. Sperati, and D.H. Busch, *J. Am. Chem. Soc.*, **99,** 2968 (1977).
12. T. Ito, M. Kato, and H. Ito, *Bull. Chem. Soc. Jpn.*, **57,** 1556 (1984).
13. *idem., ibid.*, **57,** 2634 91984).
14. *idem., ibid.*, **57,** 2641 (1984).
15. The basis sets used were the STO-3G set for ligand atoms and the [4s3p2d] contracted set for central metal atoms, respectively (see ref. 12).
16. Except for Co(III), such complexes are hypothetical.
17. L.Y. Martin, J.L. DeHayes, L.J. Zompa, and D.H. Busch, *J. Am. Chem. Soc.*, **96,** 4046 (1974).
18. So far we have not succeeded in the synthesis of *trans*-[Zn(NCS)$_2$([16]aneN$_4$)]. The [14]aneN$_4$, [15]aneN$_4$, and [16]aneN$_4$ ligands did not afford single crystals of six-coordinate Zn(II) complexes with Cl^- ligands at the axial positions.
19. M. Sugimoto, J. Fujita, H. Ito, K. Toriumi, and T. Ito, *Inorg. Chem.*, **22,** 955 (1983).
20. M. Sugimoto, H. Ito, K. Toriumi, T. Ito, *Acta Crystallogr., Sect. B*, **38,** 2453 (1982).
21. This holds mathematically until θ reaches $\tan^{-1}$ (a/b), where α adopts the maximum value. When θ exceeds $\tan^{-1}$ (a/b), α gets smaller with an increase in θ.
22. This holds always irrespective of the value of θ.
23. R.G. Pearson, *J. Chem. Educ.*, **45,** 581, 643 (1968).
24. B. Bosnich, R. Mason, P.T. Pauling, G.B. Robertson, and M.L. Tobe, *J. Chem. Soc., Chem. Commun.*, 97, (1965).
25. M.A. Poraj-Kosic, E.K. Jukhno, A.C. Anciskina, and L.M. Dikareva, *Kristallografiya*, **2,** 371 (1957). *Struc. Rep.* **21,** 407.
26. B.W Brown, and E.L. Ligafelter, *Acta Crystallogr.*, **16,** 753 (1963).
27. H. Ito, M. Kato, and T. Ito, unpublished result.
28. A. Nakahara, Y. Saito, and H. Kuroya, *Bull. Chem. Soc. Jpn.* **25,** 331 (1952).
29. K. Matsumoto, S. Ooi, and H. Kuroya, *Bull. Chem. soc. Jpn.* **43,** 1903 (1970).
30. M. Goto, K. Ohta, K. Toriumi, and T. Ito, *Acta Crystallogr., Sect. B*, **37,** 1189 (1981).
31. D.H. Busch, *Acc. Chem. Res.*, **11,** 392 (1978), and references cited therein.
32. R.I. Haines, and A. McAuley, *Coord. Chem. Rev.*, **39,** 77 (1981), and references cited therein.
33. K. Nag, and A. Chakravorty, *Coord. Chem. Rev.*, **33,** 87 (1980), and references cited therein.
34. H.N. Po, *Coord. Chem. Rev.*, **20,** 171 (1976), and references cited therein.
35. D.C. Olsen, and J. Vasilevskis, *Inorg. Chem.*, **8,** 1611 (1968).
36. F.V. Lovecchio, E.S. Gore, and D.H. Busch, *J. Am. Chem. Soc.*, **96,** 3109 (1974).
37. J.M. Palmer, E. Papaconstantinou, and J.F. Endicott, *Inorg. Chem.*, **8,** 1516 (1969).
38. D.C. Olsen, and J. Vasilevskis, *Inorg. Chem.*, **10,** 463 (1971).
39. K. Barefield, and M.T. Mocella, *Inorg. Chem.*, **12,** 2829 (1973).
40. A. Bencini, L. Fabbrizzi, and A. Poggi, *Inorg. Chem.*, **20,** 2544 (1981).

41. R.S. Drago, and E.I. Baucom, *Inorg. Chem.*, **11,** 2064 (1972).
42. W.E. Keyes, J.B.R. Dunn, and T.M. Loehr, *J. Am. Chem. Soc.*, **99,** 4527 (1977).
43. L. Fabbrizzi, *J. Chem. Soc., Chem. Commun.*, 1063 (1979).
44. E. Ziegerson, G. Ginzburg, D. Meyerstein, and L.J. Kirschenbaum, *J. Chem. Soc., Dalton Trans.*, 1243, (1980).
45. H. Cohen, L.J. Kirschenbaum, E. Zeigerson, M. Jaacobi, E. Fuchs, G. Ginsburg, and D. Meyerstein, *Inorg. Chem.*, **18,** 2763 (1979).
46. E. Zeigerson, G. Ginzburg, N. Shwartz, Z. Luz, and D. Meyerstein, *J. Chem. Soc., Chem. commun.*, 241 (1979).
47. E. Zeigerson, G. Ginzburg, J.Y. Becker, L.J. Kirschenbaum, H. Cohen, and D. Meyerstein, *Inorg. Chem.*, **20,** 3988 (1981).
48. E. Zeigerson, I. Bar, J. Bernstein, L.J. Kirschenbaum, and D. Meyerstein, *Inorg. Chem.*, **21,** 73 (1982).
49. E.S. Gore, and D.H. Busch, *Inorg. Chem.*, **12,** 1 (1973)
50. E.K. Barefield, and D.H. Busch, *J. Chem. Soc., Chem. Commun.*, 522 (1970).
51. K. Barefield, and M.T. Mocella, *J. Am. Chem. Soc.*, **97,** 4238 (1975).
52. A. Desideri, J.B. Raynor, and C.K. Poon, *J. Chem. Soc., Dalton Trans.*, 2051 (1977).
53. R.T. Haines, and A. McAuley, *Inorg. Chem.*, **19,** 719 (1980).
54. T. Ito, M. Sugimoto, K. Toriumi, and H. Ito, *Chem. Lett.*, 1477 (1980).
55. M. Yamashita, Thesis, The Kyushu Univ. (1980).
56. M.O. Kestner, A.L. Allred, *J. Am. Chem. Soc.*, **94,** 7189 (1972).
57. K. Barefield, and M.T. Mocella, *Inorg. Chem.*, **12,** 2829 (1973).
58. K.B. Mertes, *Inorg. Chem.*, **17,** 49 (1978).
59. T. Ito, H. Ito, and K. Toriumi, *Chem. Lett.*, 1101 (1981).
60. N.M. Alcock, E.H. Curson, N. Heiron, and D. Moore, *J. Chem. Soc., Dalton Trans.*, 1987 (1979).
61. J.S. Miller, and A.J. Epstein, *Prog. Inorg. Chem.*, **20,** 1 (1976).
62. M. Yamashita, Y. Nonaka, S. Kida, Y. Hamaue, and R. Aoki, *Inorg. Chim. Acta*, **52,** 43 (1981).
63. R.J.H. Clarck, M. Kurmoo, A.M.R. Galas, and M.B. Hursthouse, *Inorg. Chem.*, **20,** 4206 (1981).
64. R. Aoki, Y. Hamaue, S. Kida, M. Yamashita, T. Takemura, Y. Furuta, and A. Kawamori, *Mol. Cryst. Liq. Cryst.*, **81,** 301 (1982).
65. N. Matsumoto, M. Yamashita, S. Kida, *Bull. Chem. Soc. Jpn.*, **51,** 3514 (1978).
66. P.E. Fanwick, and J.L. Huckaby, *Inorg. Chem.*, **21,** 3067 (1982).
67. M. Tanaka, I. Tsujikawa, K. Toriumi, and T. Ito, *Acta Crystallogr., Sect. B* **B38,** 2793 (1982).
68. N. Matsumoto, M. Yamashita, I. Ueda, and S. Kida, *Mem. Fac. Sci., Kyushu Univ. Ser. C*, **11,** 209 (1978).
69. M. Yamashita, H. Ito, K. Toriumi, and T. Ito, *Inorg. Chem.* **22,** 1566 (1983).
70. *idem.*, submitted for publication in *Acta Crystallogr.*
71. M. Yamashita, and T. Ito, *Inorg. Chim. Acta*, **87,** L5 (1984).
72. K. Toriumi, K. Kanao, M. Yamashita, A. Ooyoshi, and T. Ito, manuscript in preparation.
73. M. Sugimoto, M. Nonoyama, T. Ito, and J. Fujita, *Inorg. Chem.*, **22,** 950 (1983).
74. M. Yamashita, H. Ito, and T. Ito, *Inorg. Chem.*, **22,** 2101 (1983).
75. V. Goedken, H. Ito, and T. Ito, *J. Chem. Soc., Chem. Commun.*, **1984,** 1453.
76. M. Beley, J.-P. Collin, R. Ruppert, and J.P. Sauvage, *J. Chem. Soc., Chem. Commun.*, 1315 (1984).
77. E. Kimura, A. Sakonaka, R. Machida, and M. Kodama, *J. Am. Chem. Soc.*, **104,** 4255 (1982). **23,** 4181 (1984).